

L.H. CUPIDO*[#], P.L. ŻAK**[#], N. MAHOMED*, J. LELITO**[#], G. PIWOWARSKI**[#], P.K. KRAJEWSKI**[#]

EXPERIMENTAL INVESTIGATION OF MODIFIED HEAT TREATMENT OF AK64-TYPE Al-Si-Cu SAND CAST ALLOY

EKSPERYMENTALNE BADANIA ZMODYFIKOWANEJ OBRÓBKIE CIEPLNEJ ODLEWU PIASKOWEGO ZE STOPU Al-Si-Cu TYPU AK64

In honour of Prof. Sc.D., Ph.D. Eng. Waldemar S. Wołczyński's 70th birthday

An experimental investigation was conducted to observe and analyze the microstructural evolution of phases present in the AK64 Al-Si-Cu alloy subjected to a modified T6 heat treatment (HT). The AK64 alloy¹ is the Polish alternative of the A319.0 ASM standard aluminium alloy. The modified T6 HT schedule with a higher temperature and shorter duration was applied in the solutioning process and lower quenching and higher artificial ageing temperature than the prescribed by the ASM standard were used. The cooling curves registered during the liberating of overheating and solidifying processes give important information on nucleation temperatures for the Al dendrite network, Al-Si eutectic reaction and precipitation of Cu-rich phases. Comparison of the as-cast and heat treated microstructures revealed predicted microstructural changes and also partial fragmentation of the Fe-rich phases was observed after the application of the modified HT programme.

Keywords: Aluminium Al-Si-Cu cast alloy; T6 heat treatment; Nucleation temperature; Al₂Cu and Al-Fe-Si phases

Artykuł poświęcony jest obróbce cieplnej stopu AK64, który jest odpowiednikiem stopu ASM: A319.0. W badaniach zastosowano zmodyfikowaną obróbkę cieplną T6 o podwyższonej (w stosunku do procedury T6 HT – ASM) temperaturze wyżarzania i skróconym czasie starzenia naturalnego po przesyleniu w wodzie. Obserwacje struktury stopu po obróbce cieplnej wykazały dużą zgodność ze strukturami przewidzianymi na podstawie przeprowadzonych symulacji numerycznych. Dodatkowo określono wartości temperatury odpowiadającej początkowi zarodkowania fazy α (Al), reakcji eutektycznej Al-Si oraz wydzielania z roztworu fazy bogatej w Cu. Opisano również częściową fragmentację fazy zawierającej Fe, będącą następstwem zastosowanej zmodyfikowanej obróbki cieplnej.

1. Introduction

Aluminium alloys have recently seen an increased usage in the automotive industry. This is due to the global obligation of carbon emission reduction and fuel efficiency in the transport sector. The good strength-to-weight ratio offered by Al-Si-Cu alloys is promising towards the compliance of these environmentally friendly criteria [1-3].

The use of aluminium alloys covers some parts of the vehicles, such as body made of extruded Al sheets. Furthermore, the heaviest components of the automobiles, such as cast-iron engine blocks and cylinder heads are now widely replaced with

the Al-ones. It allows to satisfy, today economic and ecological demands [4-6].

The enhanced mechanical properties are obtained when the alloy is subjected to the T6 heat treatment process, which causes microstructural changes due to the evolution of intermetallic phases [7-9]. The process involves solution heat treatment for dissolving soluble Cu-base and Mg-base phases, the homogenization of alloying additives and the spheroidisation of the eutectic silicon. It is followed by quenching to retain maximum quantity of precipitation-hardening phases in solution and a further artificial ageing process with the aim to acquire a uniform distribution of small precipitates for strength improvement [10-11].

¹ PN EN 1706: 2011

* DEPARTMENT OF MECHANICAL ENGINEERING, CAPE PENINSULA UNIVERSITY OF TECHNOLOGY, BELLVILLE, SOUTH AFRICA

** FACULTY OF FOUNDRY ENGINEERING, AGH UNIVERSITY OF SCIENCE AND TECHNOLOGY, KRAKOW, POLAND

Corresponding author: cupidol@cput.ac.za

It should be also noted that another process aimed at improving cast alloys properties is grain-refinement through melt inoculation, e.g. [12-14].

The microstructure of Al alloys castings is affected by many factors [7-8, 15-16]. Numerical modelling and simulation of the solidification process allows us to predict the microstructure of as-cast product [17-19]

The study provided practical data about the influence of the T6 heat treatment on microstructural evolution and how it affects the properties of the examined Al-Si-Cu alloy. The paper also shows how pouring temperature affects the initial nucleation, cooling rate of the casting and its properties in micro and macro scale.

2. Experimental procedures

2.1. Material and casting

An aluminium alloy with composition as indicated in Table 1 was cast to a green sand mould [20]. Three plates of section thicknesses 10 mm, 12.5 mm and 15 mm with a square area of 125 mm × 125 mm, each (Fig. 1) were produced. The Fig. 1 also shows the position of specimens cut from the plates for microscopy examinations (ballooned numbers 1 to 5).

K-type thermocouples were used to register the temperature changes during cooling and solidification processes. Two thermocouples per casting were used. One was placed at the contact plane between the mould and the casting. The other one was placed along the vertical centre line (Fig. 1) within the casting cavity, to measure the temperature of the casting.

TABLE 1

Compositions of AK64 ingot and A319.0 casting

Element	AK64 ingot, wt.%	A319.0 [2], wt.%
Si	6.07	5.5-6.5
Cu	3.75	3.0-4.0
Fe	0.59	1.0 max
Mn	0.45	0.5 max
Mg	0.23	0.1 max
Zn	0.11	1.0 max
Ti	0.05	0.25 max
Ni	—	0.35 max
Other	—	0.5
Al	balance	

Heat treatment

The standard heat treatment (HT) schedule, prescribed for this type of alloys in ASM Handbook [21] starts with solution HT at 505°C (±6°C) for 12 h duration, followed by water quenching at about 65-100°C. The final step is an aging treatment at temperature of 155°C for about 2-5 h. The HT schedule applied in this study was conducted as follows: solution heat treatment at

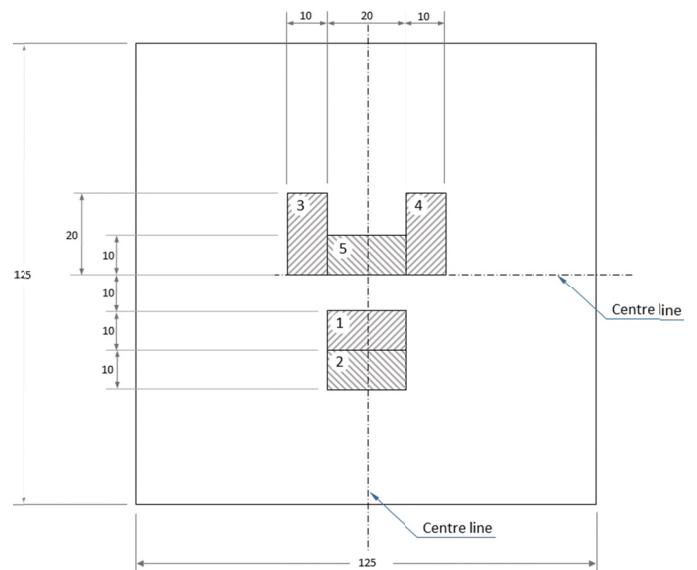


Fig. 1. Casting dimensions (in millimeters) with indication of specimen position (hatched sections). Number indicates level of priority; 1 being the highest. Five (5) was only available if the thermocouple did not reach the centre

temperature of 525°C for 6h; quenching in water of temperature 50°C; artificial ageing for 8h at temperature of 175°C; removing from furnace and final cooling to room temperature. As it can be seen the ASM program was modified to observe whether higher temperatures and shorter durations of the solutioning process would have the same effect on the microstructure and/or additional changes of the insoluble intermetallic phases.

2.2. Microscopy

Six specimens from each part of the casting different thickness were subjected to X-ray diffraction (XRD) aimed at identification of the primary, eutectic and intermetallic phases. The optical microscopy (OM) was used in analysis of the etched specimens. Additionally, scanning electron microscopy (SEM) connected with composition measurements (EDS) was conducted to more precisely identify morphology and composition of the phases which were observed in the mentioned above analyses.

3. Results

3.1. Castings soundness and cooling curves

Porosity was very severe in the casting as can be observed on the surface of specimens after their final polishing (Fig. 2). From the cooling curves (Fig. 3) it was clear that solidification time definitely had an effect on the microstructure and porosity. It was further observed that the faster cooled 10 mm casting had less porosity than the other castings with slower cooling.

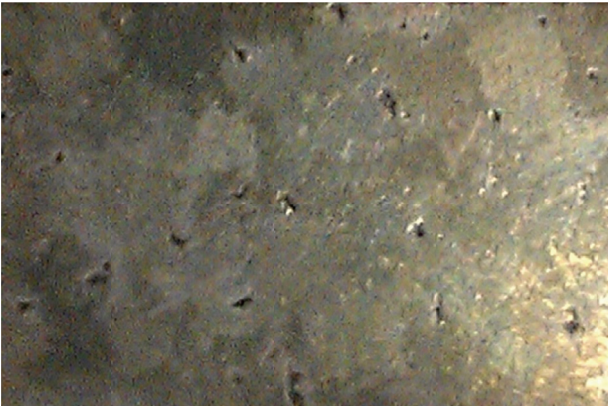


Fig. 2. Visible porosity cavities on surfaces of samples

Other important temperatures values obtain from the first derivative of the cooling curves were the following (as numbered on the graphs in Fig. 3):

- T₁: Nucleation of Al dendrite networks at about 600°C
- T₂: Nucleation of Al-Si eutectics at about 553°C
- T₃: Nucleation of Cu-rich phases at about 496°C.

3.2. Microstructural analysis

The XRD analysis (Fig. 4), performed with using XRAY-AN-software database identified the solid solution α -(Al) matrix, the eutectic silicon, the intermetallic Al₂Cu and FeSi-based

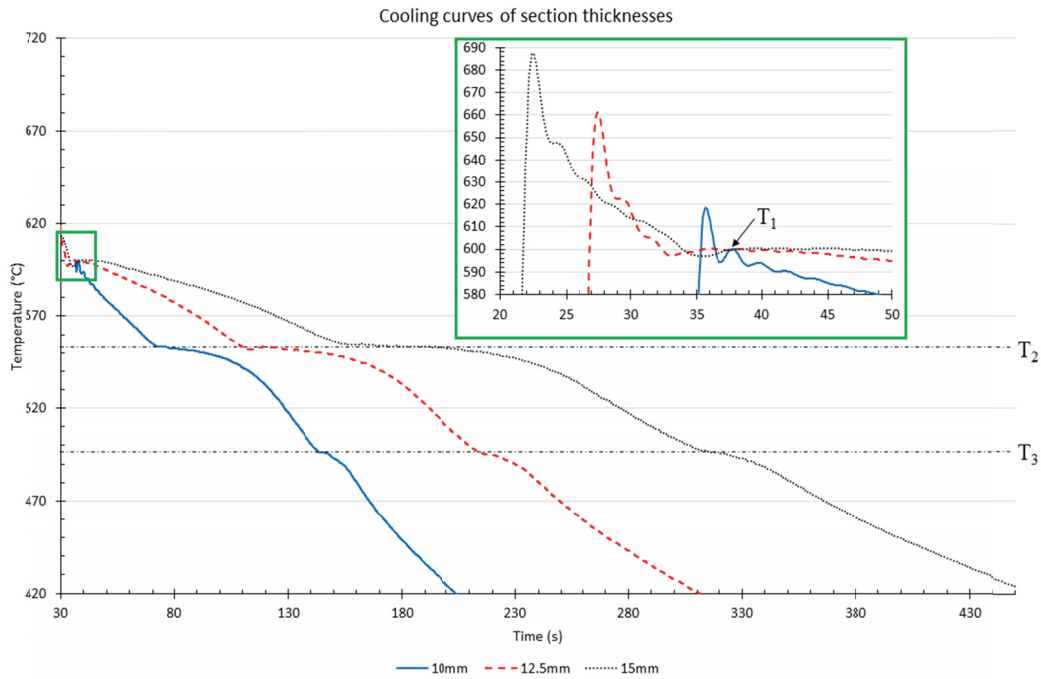


Fig. 3. Cooling curves of different-thickness samples

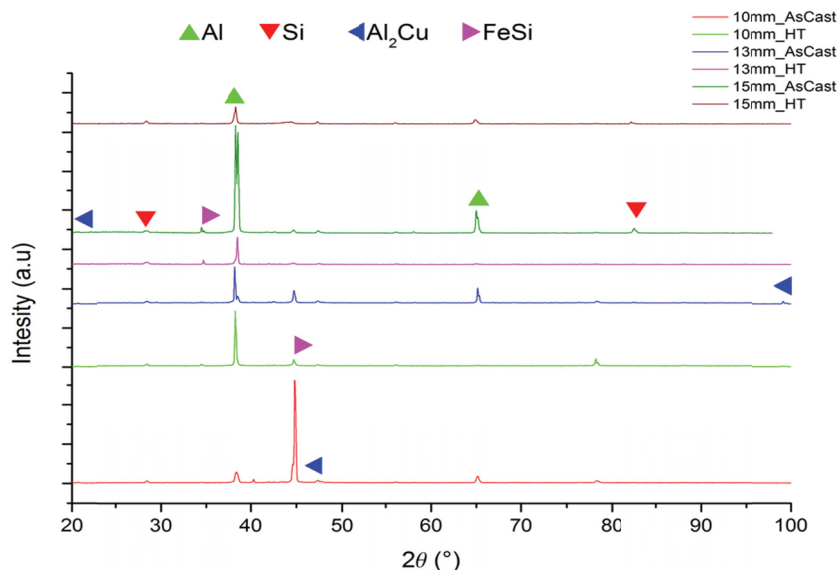


Fig.4. X-ray diffraction patterns of the examined specimens

phases. It should be noted that a reflex of the FeSi-based phase is observed very close to a high Al peak. Considering this it can be assumed that this is as reported in literature of the AlFeSi phase [22]. The optical microscopy analysis revealed the detrimental needle Si phase, as well as Al₂Cu phase in the as-cast microstructure (Fig. 5), however, the mentioned AlFeSi phase was difficult to identify. Moreover, the “Chinese-script” Fe-rich phases were identified, although with some ambiguity.

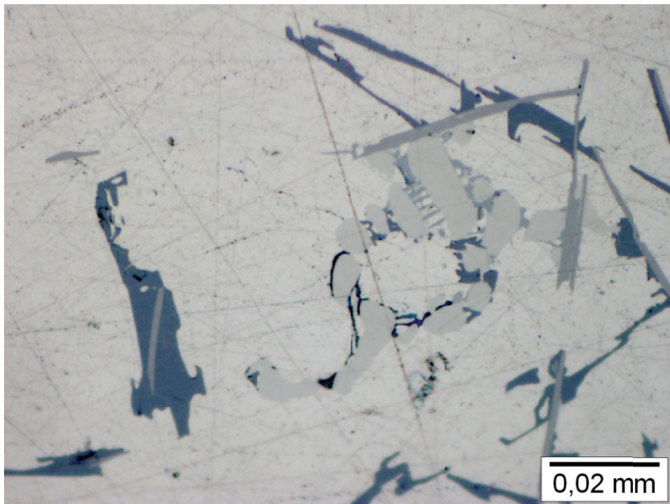


Fig. 5. Light microscopy of the as-cast microstructure; 1) Detrimental needle-like Silicon; 2) Al₂Cu phase; 3) AlFeSi phase

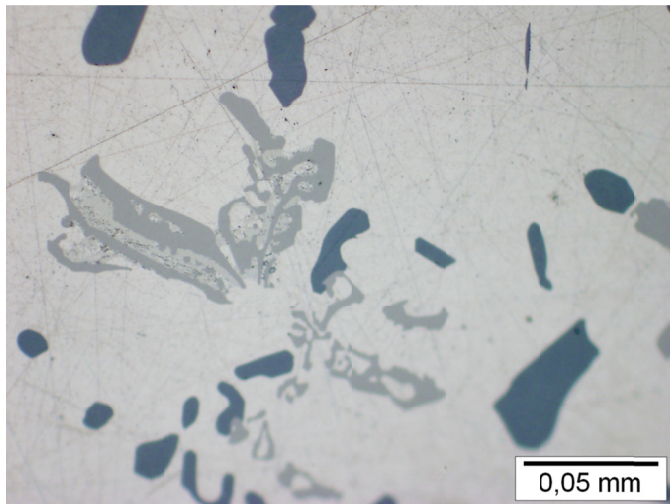


Fig. 6. Light microscopy of the microstructure of the heat treated sample; 1) Spheroidised silicon; 2) An example of probable fragmentation, segmentation and dissolution of Fe-rich phases; 3) Complex Fe-rich phase

4. Discussion and conclusions

The metallographic study revealed interesting results, both before and after the applied heat treatment. The needle-like silicon phases were clearly visible, and after heat treatment their transformation to a spheroidal shape was observed. The higher solution heat treatment temperature of 525°C, as opposed to the

recommended in literature 520°C, showed that Cu containing phases did dissolve. It was also observed that the Fe-rich phases have undergone fragmentation and dissolving processes. From this it can be concluded that the applied higher temperature of heat treatment is favourable, and that an extended period of the solutioning would dissolve it completely.

The SEM analysis revealed more complex intermetallic phases, which are rich in Fe and Mn. It was also found that Mg-containing phases manifest upon or near to Cu-rich or Fe-rich phases. Surface composition analysis of the selected areas, shown in Figures 8, indicated that dissolution of Cu occurred after heat treatment, as the Al-matrix contained an increased wt.% of the element. An indication of improved homogenisation in the casting.

It should be noted that to support these finding, further mechanical testing is required. Thus, can potentially beneficial towards industry, i.e. decrease process time which leads to cost reduction.

Acknowledgements

The authors cordially thank Professor Waldemar Wolczyński for his comments and valuable discussion.

One of the authors (L.H. Cupido) would like to express sincere gratitude for financial support under the RIFT scholarship.

The authors would like to thank Dr. E. Olejnik, MSc. B. Gracz and Dr. Z. Szklarz for performing and analysis of XRD examinations, assistance during samples preparation and microstructural analyses.

REFERENCES

- [1] W.S. Miller, L. Zhuang, J. Bottema, A.J. Wittebrood, P. De Smet, A. Haszler, A. Vierendege, Recent development in aluminium alloys for the automotive industry, *Materials Science and Engineering A* **280**, 1, 37-49 (2000).
- [2] J.G. Kaufman, E.L. Rooy, *Aluminum Alloy Castings: Properties, Processes, and Applications*, 1st ed., ASM International, , Ohio, USA (2004).
- [3] S. Gopikrishna, C.Y. Binu, Study on effects of T6 heat treatment on grain refined A319 alloy with Magnesium and Strontium addition, *International Journal on Theoretical and Applied Research in Mechanical Engineering* **2**, 3, 59-62 (2013).
- [4] A.L. Kearney, *Properties of Cast Aluminum Alloys*, in ASM Handbook, Volume 2 Properties and Selection: Nonferrous Alloys and Special-Purpose Materials, 10th ed., ASM International, 569-666 (1992).
- [5] L. Heusler, F.J. Feikus, M.O. Otte, Alloy and Casting Process Optimization for Engine Block Application, *AFS Transaction* **1**, 50, 1-9 (2001).
- [6] J. Hirsch, *Automotive Trends in Aluminium – The European Perspective*, *Materials Forum* **28**, 15-23 (2004).
- [7] W. Wolczyński, W. Krajewski, R. Ebner, J. Kloch, The use of equilibrium phase diagram for the calculation of non-equilibrium

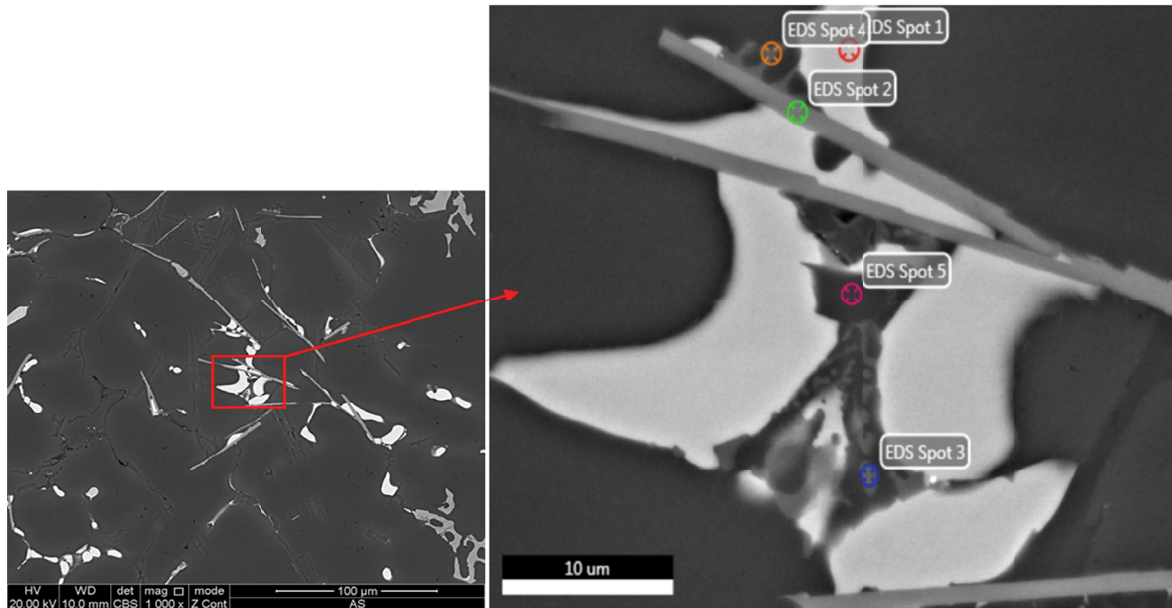


Fig. 7. SEM of as-cast microstructure; after spot analysis revealing highly complex phases (weight percent in brackets) at the EDS Spots: 1 – Al (53.35), Cu (46.65), O (0.15)Si (0.85); 2 – Al (54.16), Cu (11.13), Fe (13.35), Mg (1.18), Mn (5.01), Si (15.16); 3 – Al (53.63), Cu (14.5), Mg (15.62), Si (17.25); 4 – Al (60.97), Cu (10.89), Fe (1.02), Mg (11.7), Si (15.42); 5 – Al (29.5), Cu (3.7), Mg (0.78), Si (66.05)

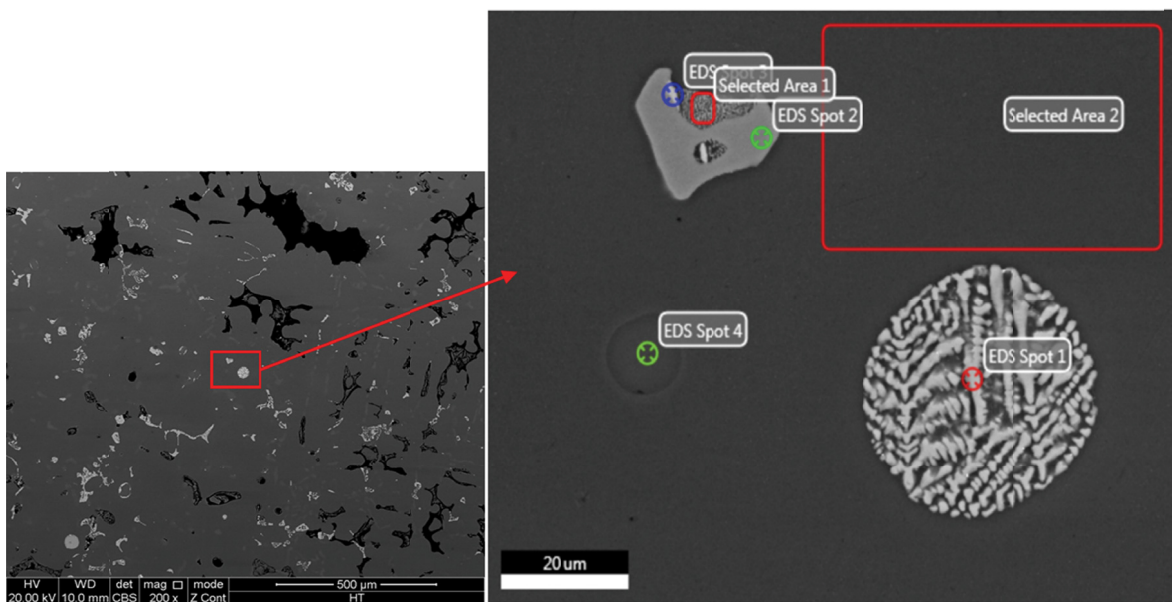


Fig. 8. SEM of the heat treated microstructure; Area analysis showing (weight percent in brackets) Cu-containing phases (Selected Area 1: Al (66.22), Cu (21.88), Mg (1.55), Si (8.34); Selected Area 2: Al (95.15), Cu (2.86), Mg (0.77), Si (1.22)) which is not noticeable under the optical micrographs. Other EDS Spots: 1 – Al (53.2), Cu (41.1), Fe (0.68), Si (4.3); 2 – Al (56.62), Cu (4.98), Fe (17.43), Mn (11.75), Si (9.22); 3 – Al (57.9), Cu (35.72), Fe (1.5), Mg (0.39), Mn (0.89), O (0.1); Si (3.51); 4 – Al (2.17), Cu (0.52), Si (97.3)

- precipitates in dendritic solidification : theory, Calphad-Computer Coupling and Phase Diagrams and Thermochemistry **25**, 3, 401-408 (2001).
- [8] W. Wołczyński, J. Kloch, R. Ebner, W. Krajewski, The use of equilibrium phase diagram for the calculation of non-equilibrium precipitates in dendritic solidification : validation, Calphad-Computer Coupling and Phase Diagrams and Thermochemistry **25**, 3, 391-400 (2001).
- [9] D. Kalisz, P.L. Žak, Modelling of solute segregation and the formation of non-metallic inclusions during solidification of a titanium-containing steel, Kovove Materialy-Metallic Materials **52**, 1-7 (2014).
- [10] A.M.A. Mohamed, F.H. Samuel, A review on the heat treatment of Al-Si-Cu/Mg casting alloys, in: Heat Treatment, Rijeka, Croatia, InTech Science, 229-246 (2012).
- [11] E. Sjölander, S. Seifeddine, Optimisation of solution treatment of cast Al-Si-Cu alloys, Materials and Design **31**, 1, S44-S49 (2010).

- [12] W. Krajewski, Phases of heterogeneous nucleation in the ZnAl25 alloy modified by Zn-Ti and Al-Ti master alloys, *Zeitschrift für Metallkunde* **87**, 645-651 (1996).
- [13] W. Krajewski, The effect of Ti addition on properties of selected Zn-Al alloys, *Physica Status Solidi A-Applied Research* **147**, 389-399 (1995).
- [14] W.K. Krajewski, A.L. Greer, P.K. Krajewski, Trends in developments of high-aluminium zinc alloys of stable structure and properties, *Archives of Metallurgy and Materials* **58**, 859-861 (2013).
- [15] P.K. Krajewski, G. Piwowarski, P.L. Żak, W.K. Krajewski, Experiment and numerical modelling the time of a plate-shape casting solidification vs. thermal conductivity of mould material, *Archives of Metallurgy and Materials* **59**, 4, 1405-1408 (2014).
- [16] W.K. Krajewski, J. Buraś, M. Żurkowski, A.L. Greer, Structure and properties of grain-refined Al – 20 wt% Zn sand cast alloy, *Archives of Metallurgy and Materials* **54**, 2, 329-334 (2009).
- [17] J.S. Suchy, J. Lelito, B. Gracz, P.L. Żak, H. Krawiec, Modelling of composite crystallization, *China Foundry* **9**, 2, 184-188 (2012).
- [18] B. Mochnacki, E. Majchrzak, Identification of macro and micro parameters in solidification model, *Bulletin of the Polish Academy of Sciences, Technical Sciences* **55**, 1, 107-113 (2007).
- [19] W.K. Krajewski, J. Lelito, J.S. Suchy, P. Schumacher, Computed tomography – a new tool in structural examinations of castings, *Archives of Metallurgy and Materials* **54**, 335-338 (2009).
- [20] L.H. Cupido, P.L. Żak, Simulation of casting technologies for Al-Si-Cu plate casting, *Archive of Foundry Engineering* **1**, 3, 11-14 (2013).
- [21] C.R. Brooks, Heat treating of nonferrous alloys, in *ASM Handbook 4, Heat Treatment*, ASM International, 1826-2124 (1991).
- [22] E. Tillova, M. Chalupova, L. Hurtalova, Evolution of the Fe-rich phases in recycled AlSi9Cu3 cast alloy during solution treatment, *Communications – Scientific Letters of University of Zilina* **10**, 4, 95-101 (2010).
- [23] J. Lelito, P.L. Żak, A.L. Greer, J.S. Suchy, W.K. Krajewski, B. Gracz, M. Szucki, A.A. Shirzadi, Crystallization model of magnesium primary phase in the AZ91/SiC composite, *Composites: Part B* **43**, 3306-3309 (2012).

Received: 20 April 2015